



# Non-smooth bursting analysis of a Filippov-type system with multiple-frequency excitations

ZIFANG QU<sup>1,2</sup>, ZHENGDI ZHANG<sup>1</sup> \*, MIAO PENG<sup>1</sup> and QINSHENG BI<sup>3</sup>

<sup>1</sup>Faculty of Science, Jiangsu University, Zhenjiang 212013, China

<sup>2</sup>School of Mathematics and Information Science, Shandong Technology and Business University, Yantai 264005, China

<sup>3</sup>Faculty of Civil Engineering and Mechanics, Jiangsu University, Zhenjiang 212013, China

\*Corresponding author. E-mail: dyzhang@ujs.edu.cn

MS received 28 February 2018; revised 11 April 2018; accepted 25 April 2018;  
published online 20 September 2018

**Abstract.** The main purpose of this paper is to explore the patterns of the bursting oscillations and the non-smooth dynamical behaviours in a Filippov-type system which possesses parametric and external periodic excitations. We take a coupled system consisting of Duffing and Van der Pol oscillators as an example. Owing to the existence of an order gap between the exciting frequency and the natural one, we can regard a single periodic excitation as a slow-varying parameter, and the other periodic excitations can be transformed as functions of the slow-varying parameter when the exciting frequency is far less than the natural one. By analysing the subsystems, we derive equilibrium branches and related bifurcations with the variation of the slow-varying parameter. Even though the equilibrium branches with two different frequencies of the parametric excitation have a similar structure, the tortuousness of the equilibrium branches is diverse, and the number of extreme points is changed from 6 to 10. Overlaying the equilibrium branches with the transformed phase portrait and employing the evolutionary process of the limit cycle induced by the Hopf bifurcation, the critical conditions of the homoclinic bifurcation and multisliding bifurcation are derived. Numerical simulation verifies the results well.

**Keywords.** Multiple frequency excitation; Filippov-type system; bursting oscillations; multisliding bifurcation.

**PACS Nos** 05.45.–a; 05.45.Pq; 05.45.Xt

## 1. Introduction

Bursting oscillation, which is originally introduced in neuronal models [1], can be found widely in low-dimensional smooth systems [2–4]. There exist many non-smooth factors which are usually represented as collision, dry friction, switch, etc. in science and engineering, and special non-smooth bifurcations found in some systems are given in [5–7]. Among the non-smooth systems, the Filippov systems have exhibited more abundant nonlinear dynamical behaviours, including complex bifurcations, sliding, chaos, etc. [8,9].

Since the real time is altered by different speeds between the subsystems, as well as the difference in quality, size and stiffness caused by different characteristics of each subsystem, the dynamics associated with multiple time scales have attracted much

attention [10–13]. Up to now, most researchers followed the modes of model analysis, approximate solution, numerical simulation and experimental analysis of systems with multiple time scales [14–16] and multistable systems [17]. It is not until Rinzel [18] introduced the slow–fast analysis method that the evolution mechanism of all kinds of dynamical behaviours could be further analysed [19]. According to this method, the whole system is divided into two subsystems, the fast subsystem and the slow subsystem, which have an effect on the forms of the spiking states (SPs) and the quiescent states (QSs) as well as related bifurcations [20].

For a classic slow–fast system, represented by

$$\begin{cases} \frac{dx}{dt} = f(x, y), & \text{fast subsystem,} \\ \frac{dy}{dt} = \varepsilon g(x, y), & \text{slow subsystem,} \end{cases} \quad (1)$$

where  $x \in R^M$ ,  $y \in R^N$ , while  $0 < \varepsilon \ll 1$ , describing the ratio of the two scales, the state vector  $y$  is considered to be a slow-varying parameter. In the standard slow-fast analysis method, by setting  $\varepsilon = 0$ , the equilibrium points as well as the bifurcation of the fast subsystem with the variation of  $y$  can be obtained, which can be employed to determine the Qs and the SPs as well as the bifurcation between the two states, while the slow subsystem can be used to reveal the modulation in the oscillations [21].

There are many reports on the periodic bursting oscillation analysis of a system with a slow variable parameter [22,23]. As there exists many kinds of multiple periodic excitations in actual dynamical systems, the analysis of the dynamical behaviour of systems with multiple frequency excitations in the time domain has aroused the scholars' interests [24], especially the systems with the combination of parametric excitation and external excitation. Since there is an order gap between the exciting frequency and the natural one, it is still a challenge to explore the bursting oscillations of the system.

Here, we explore the non-smooth bursting oscillations as well as bifurcation mechanisms in a Filippov-type system with different scales and two periodic excitations based on a coupled system consisted of Duffing and Van der Pol oscillators. The rest of the paper is organised as follows. In §2, we introduce a Filippov-type system with the combination of parametric excitation and external excitation. In §3, the equilibrium branches as well as related bifurcations and the evolution mechanism of non-smooth behaviours at non-smooth boundary are taken into account. In §4, based on numerical simulation and transformed phase portrait with the condition of two amplitudes unchanged, the bursting oscillation patterns as well as the mechanism analysis and the non-smooth evolution behaviours of the system induced by the frequency of parametric excitation are analysed. In §5, we explore the tortuous analysis of the equilibrium branches under different frequencies of parametric excitation. Finally, in §6, we conclude with a discussion of our results.

## 2. Mathematical model

As an example, a coupled system consisting of Duffing and Van der Pol oscillators is explored by introducing a bilateral diode as well as a harmonically changed electrical source. Bursting oscillations can be found when there exists an order gap between the exciting frequency and the natural one. The Filippov-type model can be written in the non-dimensional form as

$$\begin{cases} \dot{x}_1 = y_1 + w_1 + \delta \operatorname{sgn}(x_1), \\ \dot{y}_1 = -w_2 x_1 - \alpha_1 x_1^3 - \alpha_2 x_1^5 - 2\mu y_1 + \xi(x_1 - x_2), \\ \dot{x}_2 = y_2, \\ \dot{y}_2 = -\alpha_3 x_2 + (1 - x_2^2)y_2 - \xi(x_1 - x_2), \end{cases} \quad (2)$$

where  $w_1 = A_1 \cos(\Omega_1 \tau)$  and  $w_2 = A_2 \cos(\Omega_2 \tau)$  describe the external excitation and the parametric excitation, respectively, with amplitudes  $A_1, A_2$  and the frequencies  $\Omega_1, \Omega_2$ . For the meaning of other parameters, refer to [25]. The vector field is divided into two smooth regions represented as

$$D_+ = \{(x_1, y_1, x_2, y_2) | x_1 > 0\},$$

$$D_- = \{(x_1, y_1, x_2, y_2) | x_1 < 0\}$$

by the non-smooth boundary  $\Sigma = \{(x_1, y_1, x_2, y_2) | x_1 = 0\}$  defined by  $\delta \operatorname{sgn}(x_1)$  according to two non-autonomous smooth subsystems. Note that two periodic excitations are not independent of each other and by employing the slow-fast analysis method, the combination of the two exciting terms can be transformed as a function of a periodic term with single frequency, which can be regarded as a slow-varying parameter. Keep  $\Omega_1 = 0.0005$  unchanged, change the value of  $\Omega_2$  and the other parameters are taken at regular values, there exists an order gap between the frequency of two periodic excitations and the natural frequency. Then the scale effect is produced, that is the coupling between different frequencies is formed, which leads to the special oscillation patterns, such as non-smooth bursting oscillations.

## 3. Bifurcation analysis

There is a resonance relationship between the two exciting frequencies  $\Omega_1, \Omega_2$ . The external excitation can be expressed as  $w_1 = A_1 \cos(\Omega_1 \tau) = A_1 W$  and  $w_2 = A_2 \cos(\Omega_2 \tau) = A_2 f_i(W)$  ( $i = 1, 2$ ) denotes the parametric excitation with  $W = \cos(0.0005\tau)$ . Although the oscillation behaviour of the state variables in system (2) is closely related to the inherent frequency, it is modulated by the frequencies of two excitations. Since  $\Omega_1 \ll \varpi$ ,  $\Omega_2 \ll \varpi$ , we can regard  $W$  as a slow-varying parameter that leads to the so-called generalised autonomous system. That is, the whole system (2) can be considered as a coupling of the fast and slow subsystems.

The fast subsystem is

$$\begin{cases} \dot{x}_1 = y_1 + A_1 W + \delta \operatorname{sgn}(x_1), \\ \dot{y}_1 = -A_2 f_i(W)x_1 - \alpha_1 x_1^3 - \alpha_2 x_1^5 \\ \quad - 2\mu y_1 + \xi(x_1 - x_2), \\ \dot{x}_2 = y_2, \\ \dot{y}_2 = -\alpha_3 x_2 + (1 - x_2^2)y_2 - \xi(x_1 - x_2), \end{cases} \quad (3)$$

where  $i = 1, 2$ .

When  $\Omega_1 = 0.0005, \Omega_2 = 0.004,$

$$f_1(W) = 160W^4 - 256W^6 + 128W^8 - 32W^2 + 1. \tag{4}$$

When  $\Omega_1 = 0.0005, \Omega_2 = 0.005,$

$$f_2(W) = (-1 + 2W^2)(256W^8 - 512W^6 + 304W^4 - 48W^2 + 1). \tag{5}$$

The slow subsystem is  $W = \cos(0.0005\tau).$

In order to elaborate the mechanism of complex behaviours in the fast and slow coupled system, we first analyse the bifurcation of the fast subsystem. The generalised equilibrium points of the fast subsystem can be expressed as

$$\begin{aligned} \text{EQ}_+ &:= (x_1, y_1, x_2, y_2) \\ &= \left(x_0, -A_1W - \delta, \frac{\xi x_0}{\xi - \alpha_3}, 0\right), \end{aligned}$$

for  $x_0 > 0,$  implying  $x_0$  satisfies

$$\begin{aligned} -\alpha_2 x_0^5 - \alpha_1 x_0^3 - A_2 f_i(W)x_0 - \frac{\alpha_3 \xi}{-\alpha_3 + \xi} x_0, \\ -2\mu(-A_1W - \delta) = 0, \quad i = 1, 2, \end{aligned} \tag{6}$$

while

$$\begin{aligned} \text{EQ}_- &:= (x_1, y_1, x_2, y_2) \\ &= \left(x_0, -A_1W + \delta, \frac{\xi x_0}{\xi - \alpha_3}, 0\right), \end{aligned}$$

for  $x_0 < 0,$  implying  $x_0$  satisfies

$$\begin{aligned} -\alpha_2 x_0^5 - \alpha_1 x_0^3 - A_2 f_i(W)x_0 - \frac{\alpha_3 \xi}{-\alpha_3 + \xi} x_0, \\ -2\mu(-A_1W + \delta) = 0, \quad i = 1, 2. \end{aligned} \tag{7}$$

The stability of the equilibrium points can be characterised by the associated characteristic equations which are written as

$$\lambda^4 + a_1\lambda^3 + a_2\lambda^2 + a_3\lambda + a_4 = 0, \tag{8}$$

where

$$\begin{aligned} a_1 &= 2\mu - v, \quad a_2 = \alpha_3 - \xi - 2\mu v - k, \\ a_3 &= 2\mu(\alpha_3 - \xi) + kv, \quad a_4 = -k(\alpha_3 - \xi) - \xi^2, \\ k &= -5\alpha_2 x_0^4 - 3\alpha_1 x_0^2 - A_2 f_i(W) + \xi, \\ v &= 1 - \left(\frac{\xi x_0}{\xi - \alpha_3}\right)^2. \end{aligned}$$

The equilibrium points  $\text{EQ}_\pm$  are stable for  $a_1 > 0, a_1 a_2 - a_3 > 0, a_1 a_2 a_3 - a_1^2 a_4 - a_3^2 > 0, a_4 > 0,$  while the parameters meet the conditions  $a_4 = 0$  ( $a_1 > 0, a_1 a_2 - a_3 > 0, a_3 > 0$ ), that is

$$\begin{cases} [5\alpha_2 x_0^4 + 3\alpha_1 x_0^2 + A_2 f_i(W) + \xi](\alpha_3 - \xi) - \xi^2 = 0, \\ -\alpha_2 x_0^5 - \alpha_1 x_0^3 - A_2 f_i(W)x_0 - \frac{\alpha_3 \xi}{-\alpha_3 + \xi} x_0 \\ -2\mu(-A_1W \mp \delta) = 0. \end{cases} \tag{9}$$

The fold bifurcation may happen, leading to the phenomena of jumping between different equilibrium points. Another type of bifurcation may exist, which is expressed as

$$\begin{aligned} a_1 a_2 a_3 - a_1^2 a_4 - a_3^2 &= 0 \\ (a_1 > 0, a_4 > 0, a_1 a_2 - a_3 > 0), \end{aligned} \tag{10}$$

on which the Hopf bifurcation may occur.

### 4. Numerical simulations

Now fix the parameters as  $\alpha_1 = 8, \alpha_2 = 1, \alpha_3 = 1, \xi = 0.7, \mu = 0.2$  and  $\delta = -1.$  We study the dynamics as well as the mechanism and the evolution of non-smooth behaviours at non-smooth boundary when the amplitudes of the two periodic excitations are constants and the frequency of the parametric excitation is changed.

This paper mainly describes the mechanism of periodic bursting oscillations and evolutionary analysis of the non-smooth behaviours in the system with

- (i)  $\Omega_1 = 0.0005, \Omega_2 = 0.004;$
- (ii)  $\Omega_1 = 0.0005, \Omega_2 = 0.005.$

#### 4.1 Bursting oscillations for $\Omega_1 = 0.0005, \Omega_2 = 0.004$

As shown in figures 1 and 2, one periodic bursting oscillation and non-smooth evolutionary behaviours can be obtained when the amplitudes are fixed at  $A_1 = 7, A_2 = 3,$  and keeping  $\Omega_1 = 0.0005$  and  $\Omega_2 = 0.004$  unchanged.

As phase portrait on the  $(x_1, y_1)$  plane shows, the vector field of the system is divided into two smooth regions

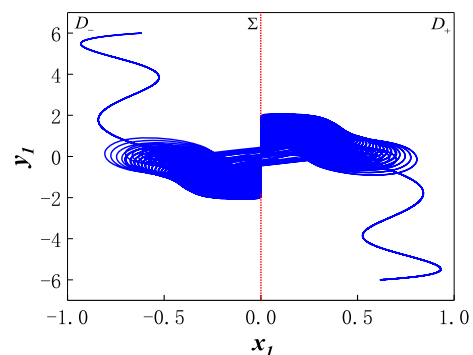


**Figure 1.** Phase portrait on the  $(x_1, y_1)$  plane for  $\Omega_1 = 0.0005$  and  $\Omega_2 = 0.004.$

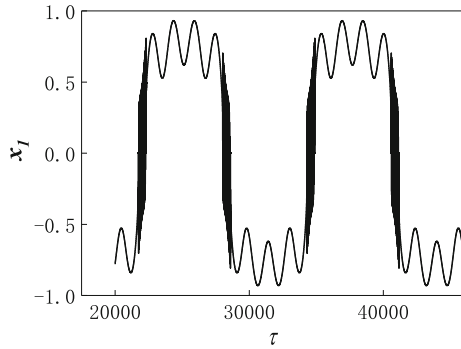


**Figure 2.** Time history of  $x_1$  for  $\Omega_1 = 0.0005$  and  $\Omega_2 = 0.004$ .

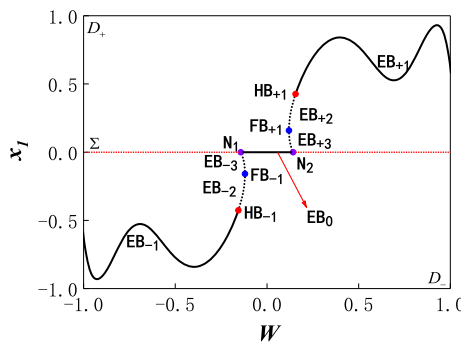


**Figure 3.** Equilibrium branches as well as bifurcations for  $\Omega_1 = 0.0005$  and  $\Omega_2 = 0.004$ .

among which the trajectory shows rich non-smooth dynamical behaviours by the non-smooth boundary  $\Sigma$ . The trajectory may slide on the boundary which frequently may cause the trajectory to exhibit periodic oscillations with alternations between SPs and Qs, or cross through the boundary and enter into another region for oscillation.

To expound the mechanism of such periodic bursting oscillation, figure 3 gives the equilibrium branches as well as the bifurcations with the variation of the slow-varying parameter. The red points in figure 3 refer to the supercritical Hopf bifurcation points, the blue points denote the fold bifurcation points, while the purple points correspond to the cross-over points between the branches and the boundary.

As is shown in equilibrium branches as well as the bifurcations, the equilibrium branches corresponding to the system are divided into seven segments by the supercritical Hopf bifurcation points  $HB_{\pm 1}(W, x_1) = (\pm 0.1562, \pm 0.4266)$ , the fold bifurcation points  $FB_{\pm 1}(W, x_1) = (\pm 0.1197, \pm 0.1592)$  and the cross-over points between the branches and the boundary, denoted by  $N_1(W, x_1) = (-0.1467, 0)$  and  $N_2(W, x_1) = (0.1467, 0)$ . Meanwhile, the dotted lines denote unstable solutions while the solid curves describe stable ones. Using the differential inclusion theory, the

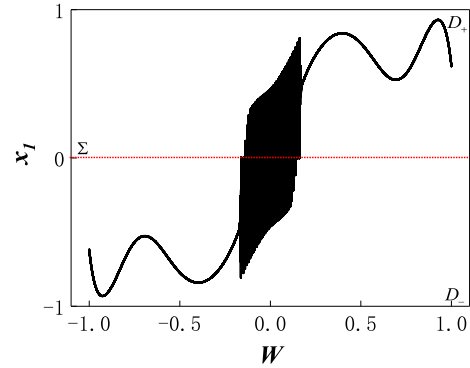


**Figure 4.** Transformed phase portrait on the  $(W, x_1)$  plane for  $\Omega_1 = 0.0005$  and  $\Omega_2 = 0.004$ .

auxiliary parameter  $q$  is introduced, and system (2) is represented by  $F$  while system (2) can be rewritten as

$$F := qF_+ + (1 - q)F_- \tag{11}$$

and the auxiliary parameter  $q$  can be represented by

$$q = \frac{-y_s - A_1 W_s + \delta}{2\delta}. \tag{12}$$

$y_s$  and  $W_s$  indicate the value of the state variable  $y$  and the slow variable parameter  $W$ , respectively, when the trajectory gets into contact with the non-smooth boundary  $\Sigma$ . Due to the nonlinear dynamical characteristics of non-smooth boundary and the theory of differential inclusions, a  $\Sigma$ -equilibrium curve appears in the equilibrium branches, as shown in figure 3.

We employ the transformed phase portrait on the  $(W, x_1)$  plane and the overlap of equilibrium branches with transformed phase portrait to better explain the mechanism of the periodic bursting oscillations (figure 4). It is found that the trajectory exhibits both SPs and Qs during a periodic bursting oscillation and the transformation of the trajectory between different SPs makes the trajectory contact with the non-smooth boundary. Furthermore, the trajectory may slide on the boundary, or cross through the boundary, or enter into another region to show special bursting oscillations (figure 5).

In order to better exhibit the oscillating forms of the trajectory in the smooth region and the bursting oscillations, figures 6–9 give the stable limit cycles generated by Hopf bifurcations due to different slow-varying parameters.

Without loss of generality, assuming the movement starts from the point  $W = -1$  in the region  $D_-$ , the trajectory may strictly move along the stable focus-type equilibrium branch  $EB_{-1}$ , showing that the system is in quiescent state  $QS_1$ . When the trajectory arrives at the Hopf bifurcation point  $HB_{-1}(W, x_1) = (-0.1562, -0.4266)$ , Hopf bifurcation occurs and the

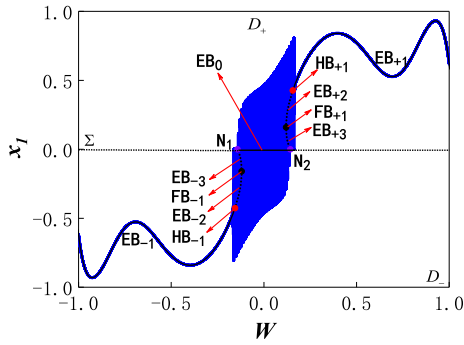


**Figure 5.** Overlap of equilibrium branches and transformed phase portrait on the  $(W, x_1)$  plane for  $\Omega_1 = 0.0005, \Omega_2 = 0.004$ .

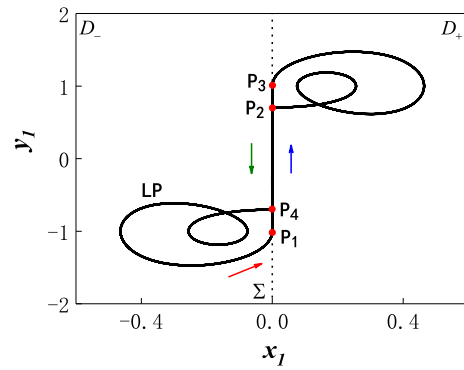


**Figure 9.** Stable limit cycle with  $W = 0$ .

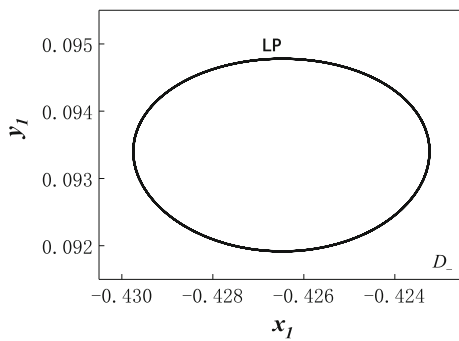


**Figure 6.** Stable limit cycle with  $W = -0.1562$ .

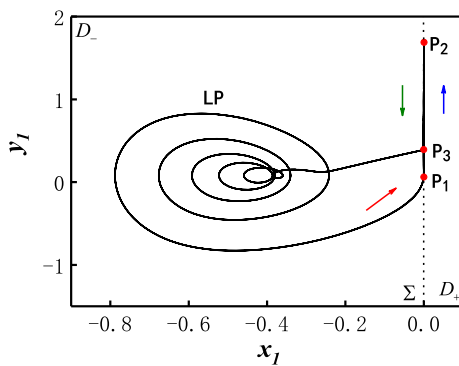


**Figure 7.** Stable limit cycle with  $W = -0.1544$ .

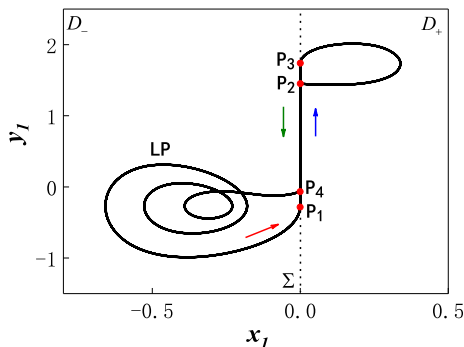


**Figure 8.** Stable limit cycle with  $W = -0.1044$ .

equilibrium point becomes unstable, which produces a stable limit cycle. As the limit cycle may be in contact with the non-smooth boundary when the slow-varying parameter changes, the dynamical behaviours will change obviously due to the influence of non-smooth factors.

We take the limit cycle shown in figures 6–9 as an example. The supercritical Hopf bifurcation point  $HB_{-1}(W, x_1) = (-0.1562, -0.4266)$  appears when  $W$  is changed to  $W = -0.1562$ . The limit cycle shown in figure 6 is completely in the smooth area  $D_-$  and does not contact with the non-smooth boundary  $\Sigma$  when it oscillates around the unstable focus-type equilibrium branches  $EB_{-2}$  and  $EB_{-3}$  in counter-clockwise direction.

The amplitudes of the oscillations gradually increase with the growth of the slow-varying parameter  $W$ . Till  $W$  is up to the value  $W = -0.1544$ , the limit cycle contacts with the non-smooth boundary  $\Sigma$  in the direction of the red arrow at the point  $P_1(x_1, y_1) = (0, 0.0560)$ . Soon it slides along the boundary in the direction of the blue arrow until it arrives at the point  $P_2(x_1, y_1) = (0, 1.6878)$ , then it continues to move in the direction of the green arrow till it arrives at the point  $P_3(x_1, y_1) = (0, 0.3959)$  and leaves the boundary immediately. That is, after oscillating from the smooth region  $D_-$  into the boundary and sliding along it for a period of time, the trajectory escapes from the boundary, then returns to the smooth region again and continues to move. Therefore, the slow variable parameter  $W = -0.1544$  corresponds to the homoclinic bifurcations of the Filippov-type generalised autonomous system.

When the slow-varying parameter  $W$  increases to  $W = -0.1044$ , the limit cycle comes to the boundary at the point  $P_1(x_1, y_1) = (0, -0.3067)$  and slides along the boundary in the direction of the blue arrow until it gets to the point  $P_2(x_1, y_1) = (0, 1.4506)$ , then it passes through the boundary  $\Sigma$  immediately and enters into the smooth region  $D_+$ . After oscillating for a while in the smooth region  $D_+$ , the limit cycle

comes back to the boundary at the point  $P_3(x_1, y_1) = (0, 1.7431)$  and continues to move along the boundary in the direction of the green arrow. When the limit cycle reaches the point  $P_4(x_1, y_1) = (0, -0.0622)$ , it keeps on oscillating in the smooth region  $D_-$ . Therefore, the slow variable parameter  $W = -0.1044$  corresponds to the multisliding bifurcations of the Filippov-type generalised autonomous system.

Figure 9 gives symmetrical oscillation patterns of the trajectory when  $W$  changes to 0. The oscillation patterns of the trajectory are similar to those of the previous motion. The limit cycle gets to the boundary at the point  $P_1(x_1, y_1) = (0, -1.0395)$ , and shows sliding motion on the boundary in the direction of the blue arrow until it arrives at the point  $P_2(x_1, y_1) = (0, 0.6990)$ , then it slides through the boundary  $\Sigma$  quickly and goes into the smooth region  $D_+$  to oscillate for a short time. Then the trajectory goes back to the boundary at the point  $P_3(x_1, y_1) = (0, 1.0395)$  with time and still slides along the boundary in the direction of the green arrow until it comes to the point  $P_4(x_1, y_1) = (0, -0.6990)$ . According to the above analysis, we can conclude that the trajectory oscillates symmetrically in both the regions  $D_+$  and  $D_-$ .

The slow-varying parameter  $W$  then increases with time. Meanwhile, the amplitudes of the oscillations constantly increase until  $W$  gets the maximum value at  $W = 1$ . The trajectory may finally settle down to the stable equilibrium curve  $EB_{+1}$  and moves almost strictly along it with further increase of  $W$  to form QS until it arrives at the supercritical Hopf bifurcation point  $HB_{+1}(W, x_1) = (0.1562, 0.4266)$ , at which the Hopf bifurcation occurs, leading to the generation of the limit cycle. It is found that the limit cycle presents a similar and symmetrical evolutionary behaviour with the limit cycle generated by the supercritical Hopf bifurcation point  $HB_{-1}(W, x_1) = (-0.1562, -0.4266)$ . The slow-varying parameter  $W$  gradually decreases with the increasing time, and the trajectory may finally converge on the stable equilibrium curve  $EB_{-1}$  and moves almost strictly to follow it. When the trajectory arrives at the starting point  $W = -1$ , one period of the bursting oscillations is finished.

#### 4.2 Bursting oscillations for $\Omega_1 = 0.0005$ , $\Omega_2 = 0.005$

As figures 10 and 11 show, one period of the bursting oscillations and the non-smooth evolutionary behaviours also can be obtained when the amplitudes are fixed at  $A_1 = 7$ ,  $A_2 = 3$  with  $\Omega_1 = 0.0005$ ,  $\Omega_2 = 0.005$ .

The trajectory may slide along the boundary which frequently causes the trajectory to exhibit periodic oscillations with alternations between SPs and QSSs, or cross

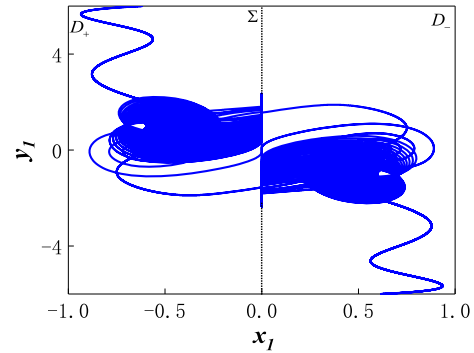


**Figure 10.** Phase portrait on the  $(x_1, y_1)$  plane for  $\Omega_1 = 0.0005$ ,  $\Omega_2 = 0.005$ .

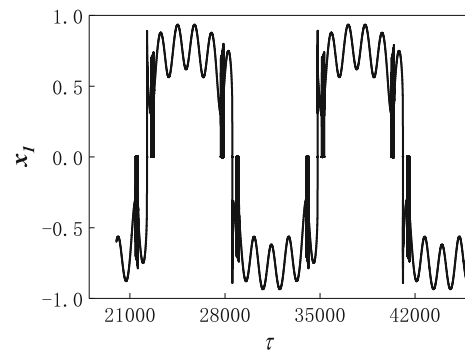


**Figure 11.** Time history of  $x_1$  for  $\Omega_1 = 0.0005$ ,  $\Omega_2 = 0.005$ .

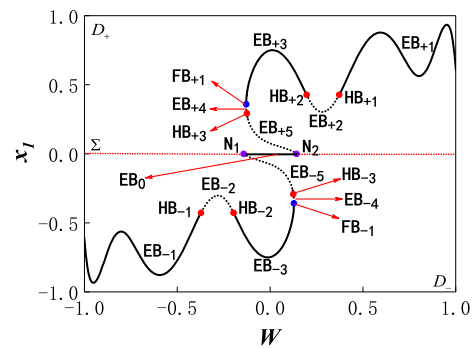


**Figure 12.** Equilibrium branches as well as bifurcations for  $\Omega_1 = 0.0005$ ,  $\Omega_2 = 0.005$ .

through the boundary, or get into another region to show the special bursting oscillations.

To expound the mechanism of such periodic bursting oscillations, figure 12 gives the equilibrium branches as well as the bifurcations with the variation of the slow-varying parameter. The red points in figure 12 refer to the supercritical Hopf bifurcation points, the blue points denote the fold bifurcation points, while the purple points correspond to the cross-over points between the branches and the boundary.

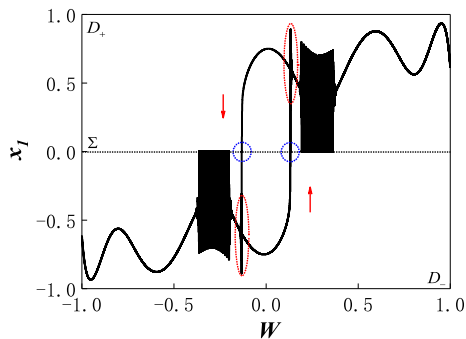


**Figure 13.** Transformed phase portrait on the  $(W, x_1)$  plane for  $\Omega_1 = 0.0005, \Omega_2 = 0.005$ .

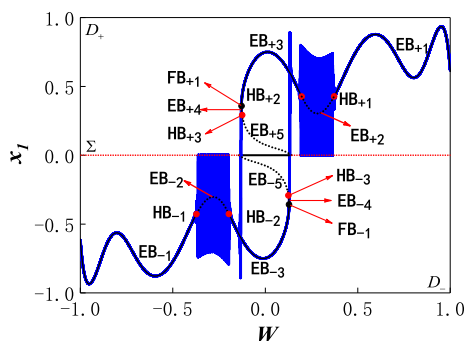


**Figure 14.** Overlap of equilibrium branches and transformed phase portrait on the  $(W, x_1)$  plane for  $\Omega_1 = 0.0005, \Omega_2 = 0.005$ .

As shown, the equilibrium branches corresponding to the system are divided into 11 segments by the supercritical Hopf bifurcation points:  $HB_{\pm 1}(W, x_1) = (\pm 0.3724, \pm 0.4274)$ ,  $HB_{\pm 2}(W, x_1) = (\pm 0.1968, \pm 0.4268)$ ,  $HB_{\pm 3}(W, x_1) = (\mp 0.1253, \pm 0.2922)$ , the fold bifurcation points  $FB_{\pm 1}(W, x_1) = (\pm 0.1286, \mp 0.3584)$ , and the intersection of the trajectory and the boundary, denoted as  $N_1(W, x_1) = (-0.1467, 0)$  and  $N_2(W, x_1) = (0.1467, 0)$ . Meanwhile, the dotted curves denote the unstable solutions while the solid lines describe the stable ones, respectively. Compared to the case of  $\Omega_1 = 0.0005, \Omega_2 = 0.004$  discussed earlier, the tortuousness of the equilibrium curve is increased, and the number of the corresponding extreme points is also changed from 6 to 10.

We use the transformed phase portrait on the  $(W, x_1)$  plane (figure 13), the overlap of equilibrium branches with the transformed phase portrait (figure 14) and locally enlarged part of the transformed phase portrait on the  $(W, x_1)$  plane (figures 15–18) to better elaborate the mechanism of the periodic bursting oscillations.

In general, assuming that the trajectory starts from the point  $W = -1$  in the region  $D_-$ , it may strictly move along the stable focus-type equilibrium branch  $EB_{-1}$ , showing that the system is in the quiescent state

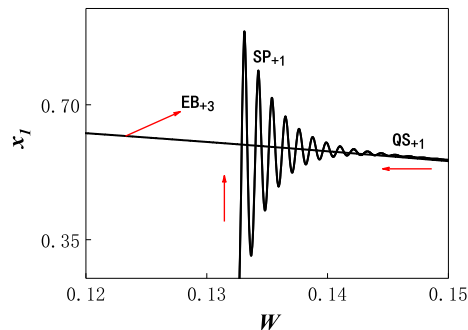


**Figure 15.** Locally enlarged part one of the transformed phase portrait on the  $(W, x_1)$  plane for  $\Omega_1 = 0.0005, \Omega_2 = 0.005$ .

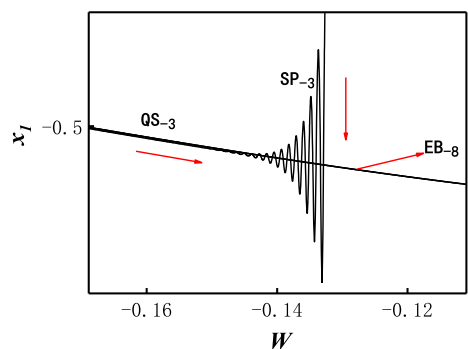


**Figure 16.** Locally enlarged part two of the transformed phase portrait on the  $(W, x_1)$  plane for  $\Omega_1 = 0.0005, \Omega_2 = 0.005$ .

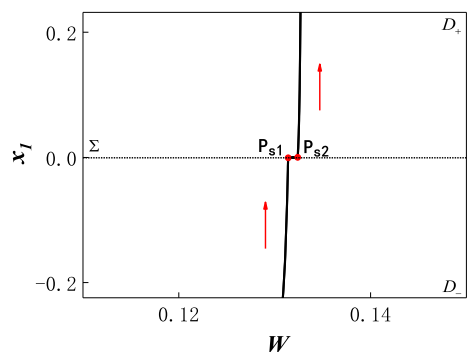


**Figure 17.** Locally enlarged part three of the transformed phase portrait on the  $(W, x_1)$  plane for  $\Omega_1 = 0.0005, \Omega_2 = 0.005$ .

$QS_1$ . When the trajectory arrives at the Hopf bifurcation point  $HB_{-1}(W, x_1) = (-0.3724, -0.4274)$ , the Hopf bifurcation which can bring a stable limit cycle occurs and the equilibrium point becomes unstable. As the limit cycle can get in touch with the non-smooth boundary  $\Sigma$  when the slow-varying parameter alters, the evolutionary behaviours will change obviously due to the influence of non-smooth factors.

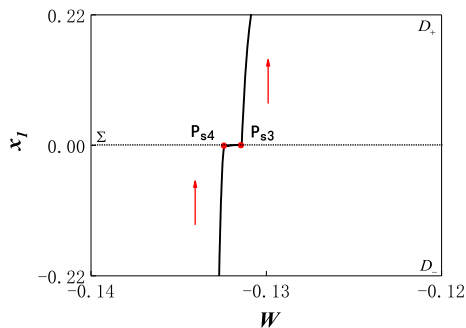


**Figure 18.** Locally enlarged part four of the transformed phase portrait on the  $(W, x_1)$  plane for  $\Omega_1 = 0.0005, \Omega_2 = 0.005$ .

The trajectory exhibits different patterns of the trajectory with  $\Omega_1 = 0.0005, \Omega_2 = 0.004$  when it oscillates around the unstable focus-type equilibrium branch  $EB_{-2}$  in counter-clockwise direction. Initially, the limit cycle is completely in the smooth region without entering into the non-smooth boundary. After a period of time, the limit cycle gets in touch with the boundary and then slides along the boundary, resulting in homoclinic bifurcations. Then the trajectory begins to oscillate, showing the spiking state  $SP_{-1}$ . The slow-varying parameter  $W$  increases with time. Meanwhile, the amplitudes of the oscillations constantly decrease. The trajectory settles down to the stable equilibrium curve  $EB_{-3}$  finally and moves almost strictly along it with further increase of  $W$  to form the quiescent state  $QS_{-2}$  until it arrives at the fold bifurcation point  $FB_{-1}(W, x_1) = (-0.1286, 0.3584)$ , at which fold bifurcation occurs, leading to the jumping phenomenon of the trajectory and showing the spiking state  $SP_{-2}$ .

Later, the trajectory comes to the boundary at the point  $P_{s1}(W, x_1) = (0.1314, 0)$  and slides along the boundary in the direction of the red arrow until it arrives at the point  $P_{s2}(W, x_1) = (0.1324, 0)$ , then it passes through the boundary  $\Sigma$  quickly and moves to the smooth region  $D_+$  for oscillation, showing the spiking state  $SP_{+1}$ .

The slow-varying parameter  $W$  then increases with time. Meanwhile, the amplitudes of oscillations continue to decrease. The trajectory may finally stabilise on the stable equilibrium curve  $EB_{+3}$ , showing the quiescent state  $QS_{+1}$ . The trajectory reaches the supercritical Hopf bifurcation point  $HB_{+2}(W, x_1) = (0.1968, 0.4268)$ , at which the Hopf bifurcation occurs again, leading to the generation of the limit cycle. The limit cycle presents a similar and symmetrical evolutionary behaviour with the limit cycle generated by the supercritical Hopf bifurcation point  $HB_{-1}(W, x_1) = (-0.3724, -0.4274)$ , that is homoclinic bifurcations of the Filippov-type generalised autonomous system.

The time continues to increase, and as the value of the slow-varying parameter  $W$  raises, the amplitudes of oscillations continuously reduce. The trajectory may continue to move almost strictly following the stable equilibrium curve  $EB_{+1}$ , showing the quiescent state  $QS_{+2}$ . When  $W$  is equal to the extreme point  $W = 1$ , the trajectory finally converges on the stable equilibrium curve  $EB_{+1}$ . With time, the slow-varying parameter  $W$  decreases continuously, showing that the system is in the quiescent state  $QS_{+3}$ . When the trajectory gets to the Hopf bifurcation point  $HB_{+1}(W, x_1) = (0.3724, 0.4274)$ , Hopf bifurcation occurs and the equilibrium point becomes unstable again. The trajectory is relative to the previous motion until it returns back to the starting point and completes one period of non-smooth bursting oscillations.

### 5. The evolution of the equilibrium branches in two cases

The equilibrium branches in two cases are shown in figures 19 and 20. We find that, although the equilibrium curves exhibit similar structures, the tortuous degree enhances with the evolution of the parametric excitation frequency, and the number of extreme points also increases, while the transformation phase portrait with the corresponding bursting oscillations becomes complicated. The cause of this phenomenon is that there exists an order gap in two periodic excitations. We take  $\Omega_1 = 0.0005, \Omega_2 = 0.004$  as an example. When one vector with a small frequency moves about one period, the other vector with a large frequency has moved eight periods, and the coupling happens to form a new period.

To describe the change in the number of extreme points corresponding to the equilibrium branches, figures 21 and 22 give the evolution of extreme points in two cases, where the black point corresponds to the extreme point of the equilibrium branches in figures 19 and 20.

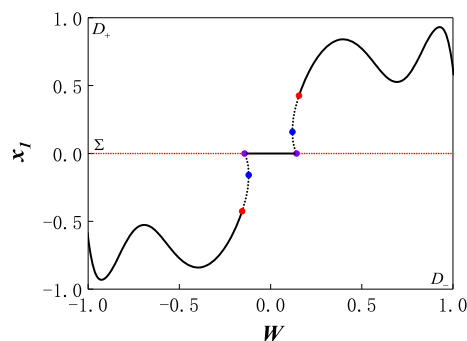


**Figure 19.** Equilibrium branches as well as bifurcations for  $\Omega_1 = 0.0005, \Omega_2 = 0.004$ .



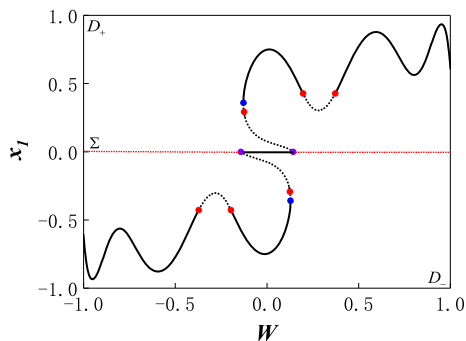


**Figure 20.** Equilibrium branches as well as bifurcations for  $\Omega_1 = 0.0005, \Omega_2 = 0.005$ .

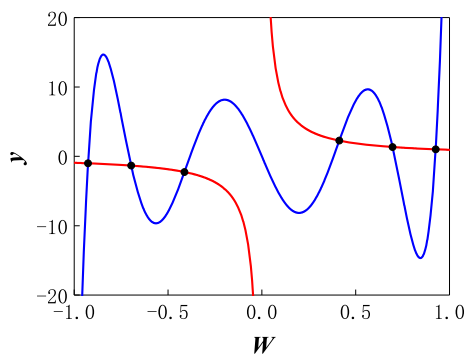


**Figure 21.** Variation of extreme points with  $\Omega_1 = 0.0005, \Omega_2 = 0.004$ .

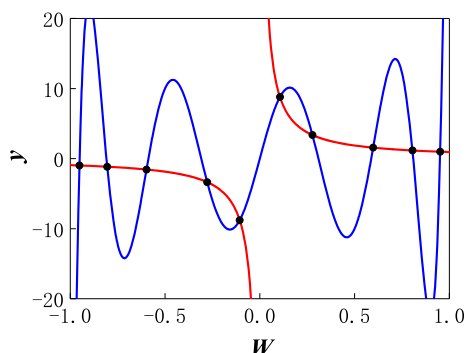


**Figure 22.** Variation of extreme points with  $\Omega_1 = 0.0005, \Omega_2 = 0.005$ .

As figure 21 shows,  $\Omega_1 = 0.0005, \Omega_2 = 0.004$ , the number of extreme points about the equilibrium branches is 6, when  $\Omega_1 = 0.0005, \Omega_2 = 0.005$ , the number of extreme points increases to 10. Comparing figures 19 and 20 with figures 21 and 22, we find that the number of extreme points in black is consistent with the number of extreme points in the equilibrium branches, and the coordinates of the extreme points also coincide with those shown in the equilibrium branches. For  $\Omega_1 = 0.0005, \Omega_2 = 0.004$ , the coordinates of the points corresponding to the maximum are  $W_{\pm 1} =$

$\pm 0.4126, W_{\pm 2} = \pm 0.6964, W_{\pm 3} = \pm 0.9261$ , for  $\Omega_1 = 0.0005, \Omega_2 = 0.005$ , the coordinates of the extreme points are  $W_{\pm 1} = \pm 0.1062, W_{\pm 2} = \pm 0.2776, W_{\pm 3} = \pm 0.5979, W_{\pm 4} = \pm 0.8050, W_{\pm 5} = \pm 0.9520$ .

### 6. Conclusions

Along with the analysis of the non-smooth bursting oscillation mechanism of Filippov-type system with multiple frequency excitations, other excitations are expressed as functions of some single excitation which can be regarded as a slow-varying parameter by algebraic transformation. By using the fast–slow analysis method, we get the evolutionary mechanism of the equilibrium branches as well as the related bifurcations in the fast subsystem with slow-varying parameters when the two excitation amplitudes are constants. The external excitation frequency remains unchanged and the parametric excitation frequency is altered. According to the transformed phase portrait on the  $(W, x_1)$  plane and the evolution of stable limit cycle with different slow-varying parameters, we find multisliding bifurcations and various multisliding oscillations, which make bursting oscillation mechanism of the system more complicated and the non-smooth dynamical behaviour characteristics more obvious. By comparing the equilibrium branches as well as the related bifurcations with two different parametric frequencies, we find that although the equilibrium curves exhibit similar structures, the tortuous degree enhances with the change of the parametric frequency. The number of extreme points also increases, and the transformation phase portrait of the corresponding bursting oscillations becomes more complicated. All the above results are verified by the numerical simulation.

It must be pointed out that this paper analyses the phenomena produced by the system when the value of  $\Omega_1$  remains unchanged and the value of  $\Omega_2$  is changed. If the value of  $\Omega_2$  is a constant and the value of  $\Omega_1$  is altered, the system may have different nonlinear dynamical behaviours. We will discuss the situation in the other way. It provides theoretical basis and technical guidance for dynamic characteristics analysis, parameter identification, model demonstration and optimisation design of nonlinear dynamic system. And it also has certain engineering application value.

### Acknowledgements

This work was supported by the Key Program of the National Natural Science Foundation of China (Grant No. 11632008) and the National Natural Science Foundation of China (Grant No. 11472116).

## References

- [1] E M Izhikevich, *Biosystems* **67**, 95 (2002)
- [2] Z D Zhang, B B Liu and Q S Bi, *Nonlinear Dyn.* **79**, 195 (2015)
- [3] H Simo and P Wofo, *Mech. Res. Commun.* **38**, 537 (2011)
- [4] S Adly, *J. Math. Anal. Appl.* **322**, 1055 (2010)
- [5] X R Li, D H Zhang, F Zhang and P Zhang, *Ecol. Indic.* **83**, 404 (2017)
- [6] R Rocha, J Ruthiramoorthy and T Kathamuthu, *Nonlinear Dyn.* **88**, 2577 (2017)
- [7] R I Leine and D H V Campen, *Eur. J. Mech. – A/Solids* **25**, 595 (2006)
- [8] P Kowalczyk and M di Bernardo, *Physica D* **204**, 204 (2005)
- [9] M di Bernardo, A Nordmark and G Olivar, *Physica D* **237**, 119 (2008)
- [10] G V Savino and C M Formigli, *Biosystems* **97**, 9 (2009)
- [11] A Sherman, J Rinzel and J Keizer, *J Biophys.* **54**, 411 (1988)
- [12] E L Lameu, F S Borges, R R Borges, A M Batista, M S Baptista and R L Viana, *Commun. Nonlinear Sci.* **34**, 45 (2016)
- [13] X Y Hu, C G Liu, L Liu, J K Ni and S L Li, *Nonlinear Dyn.* **84**, 2317 (2016)
- [14] Q S Bi, R Zhang and Z D Zhang, *Appl. Math. Comput.* **243**, 482 (2014)
- [15] G A Chumakov, N A Chumakova and E A Lashina, *Chem. Eng. J.* **282**, 11 (2015)
- [16] K Tsaneva-Atanasova, H M Osinga, T Riess and A Sherman, *J. Theor. Biol.* **264**, 1133 (2010)
- [17] M Alikhan, M Nag and S Poria, *Pramana – J. Phys.* **89**: 19 (2017)
- [18] J Rinzel, *Bull. Math. Biol.* **52**, 5 (1990)
- [19] X J Han, Q S Bi, P Ji and J Kurths, *Phys. Rev. E* **92**, 012911 (2015)
- [20] Z D Zhang, Y Liu, S Z Zhang and Q S Bi, *Acta Phys. Sin.* **66**, 020501 (2016)
- [21] E M Izhikevich, *Int. J. Bifurc. Chaos* **10**, 1171 (2000)
- [22] T Y Wu, X K Chen, Z D Zhang, X F Zhang and Q S Bi, *Acta Phys. Sin.* **66**, 110501 (2017)
- [23] Q S Bi and X K Chen, *Nonlinear Dyn.* **85**, 2233 (2016)
- [24] B Pal, D Dutta and S Poria, *Pramana – J. Phys.* **89**: 32 (2017)
- [25] X K Chen, S L Li, Z D Zhang and Q S Bi, *Sci. China Tech. Sci.* **60**, 289 (2017)